

Local and Average Glass Transitions in Polymer Thin Films

Jane E. G. Lipson^{*,†} and Scott T. Milner^{*,‡}

[†]Department of Chemistry, Dartmouth College, Hanover, New Hampshire 03755, United States, and

[‡]Department of Chemical Engineering, The Pennsylvania State University, University Park, Pennsylvania 16802, United States

Received May 18, 2010; Revised Manuscript Received September 15, 2010

ABSTRACT: In the companion paper (DOI 10.1021/ma101098d), we presented a quantitative theory for the suppression of the glass transition in a thin polymer film. Our delayed glassification (DG) model follows a proposal by de Gennes that free volume can be transmitted from surface to film interior via kinks transported along molecular strands or loops. In this paper, we use the DG model to predict the effects of molecular weight and film thickness on the film-averaged glass transition for a polystyrene sample. Our predictions for both freestanding and supported films of polystyrene illustrate that the DG model is able to account for some, but not all, of the experimental trends. This leads us to confront a number of issues, including how to average local glass transitions to yield a sample value as well as how to rationalize the nature of the molecular weight dependence for transitions in the thinnest freestanding films.

1. Introduction

Experimental evidence for the dramatic suppression of the glass transition of a polymeric film in the vicinity of a free surface (and far from any substrate) has been available for close to a decade. Yet no quantitative, predictive model has been developed to account for these results. In the companion paper (DOI 10.1021/ma101098d), we presented a theoretical approach having generational roots in suggestions made some years ago by de Gennes.^{1,2} The underlying physical picture is that chains at the surface can pick up kinks of free volume that may translate along the chain into the film and help to plasticize layers which are relatively (on the scale of tens of nanometers) remote from the free volume source, e.g., at the air interface. The source is also the sink, and so the kinks travel along polymeric loops. Translation of a kink along a loop takes time, and will therefore only help to lower the local glass transition (and thereby delay glassification) relative to the bulk if the travel time is less than the bulk relaxation time at the bulk glass transition temperature.

There are several essential elements of our delayed glassification (DG) model. We assume that the local segmental relaxation times obey the well-known Williams–Landel–Ferry (WLF) temperature dependence,³ which leads to that same functional dependence on T for $N^*(T)$, the longest effective loop length:

$$N^*(T) = N^*e^{c(T - T_g^b)/(T - T_0)}, \quad T \leq T_g^b \quad (1)$$

in which the longest effective loop length at the bulk glass transition N^* , c , and T_0 are adjustable parameters.

We also use Gaussian statistics for the loops in order to obtain a relatively simple result for the probability that a segment a distance z away from the interface is on a fast loop. For this latter analysis, we consider two scenarios: that a loop is made slow by a single slow segment or that the cumulative effect of moderately sluggish segments may cause a loop to become slow. The two cases differ noticeably in mathematical complexity, but marginally in

resulting predictions. We therefore proceed here with the simpler of the two pictures, that of slowness being induced via the existence of a slow segment.

Development of the DG model also requires a condition for the transition to local glassiness, i.e., a value for the critical probability, p_c . For this we applied the condition used in our earlier percolation work,⁴ viz. that coordinated slowing down of a local region required at least some limited connection between the site in question and neighboring sites. We settled on a value for p_c of the inverse of a local “coordination” number; however, we noted then, and repeat here, that our results are not particularly sensitive to this choice. In this paper we apply the DG model, for the case of both finite and infinite molecular weight polymer, to predict the local glass transition as a function of film thickness for both a semi-infinite supported and a freestanding film. In the semi-infinite case the only interface is that of the free surface; the effect of substrate is not included.

While it would be interesting to test our predictions for local T_g against experimental data, such results are not yet available, although some experiments come closer than others (as will be discussed below). In order to compare directly with experiment we shall have to consider how to translate from a set of local T_g values to a prediction for the expected T_g of a film having some experimentally manageable thickness. Before undertaking such a comparison it is useful to consider what the experimental measurements track in the course of detecting a glass transition.

A variety of techniques, some of which were noted in the companion paper (DOI 10.1021/ma101098d), have been used to probe the thickness dependence of the glass transition in a thin film. For example, measurements such as dielectric relaxation^{5,6} and Brillouin scattering^{7–9} are sensitive to slowing down of the local dynamics as the glass transition is approached. Signature responses from local modes sum over the sample being probed in order to produce an overall signal. Another class of techniques yields information about the change in height, or density, of a sample as a function of temperature, exploiting the fact that the thermal expansion coefficient changes dramatically as a system goes from melt to glass. Methods such as ellipsometry^{8,10–18} and X-ray reflectivity^{10,19–21} fall into this class, and in all cases, the

*To whom correspondence should be addressed. E-mail: (J.E.G.L.) jane.e.g.lipson@dartmouth.edu; (S.T.M.) stm9@psu.edu.

measured signal represents an average over the total sample thickness.

Also in this category is a fluorescence labeling technique developed by Torkelson and co-workers^{22–28} (see also references in ref 24), whereby selectively labeled layers of interest in a thin film may serve to report on the glass transition. The fluorescence probes, which are uniformly distributed throughout the layer of interest, emit a cumulative signal which is sensitive to local changes in density. The experiment therefore essentially detects a change in sample height, or thickness, with changing temperature, averaged over the thickness of the reporting layer. The result is a layer-averaged glass transition, with the added control of being able to label the thickness and position of the layer within the film.

As noted above, experimental measurements of T_g for a film of a given thickness represent an average. Even the fluorescence labeling results report a value which is averaged, albeit only over the labeled portion of the sample. Figure 5 of the companion paper (DOI 10.1021/ma101098d) illustrates how the local glass transition may be expected to vary within a film of a given thickness for a freestanding film. The simplest route to an average T_g would be to integrate over the relevant profile and then divide by the total thickness. The result is that each local transition is weighted equally, and is what we refer to as the “democratic average”.

While both conceptually and arithmetically simple, the democratic average does not capture what the experimental data show for freestanding films, which is a very dramatic reduction of film T_g from the bulk value as film thickness is decreased. For example, the study by Dalnoki-Veress et al.¹⁵ on freestanding films of polystyrene (PS) having molecular weights ranging between 3.50×10^5 g/mol and 9.00×10^6 g/mol shows that for a sample of 7.67×10^5 g/mol the film T_g drops from the bulk by 60 K as the sample thickness decreases from 65 to 40 nm. For a sample of 6.68×10^6 g/mol the drop in transition temperature is 80 K as the film thickness changes from roughly 85 nm to 65 nm. Overall, the data reveal that film T_g values decrease abruptly from the bulk value at thicknesses which have a rather weak molecular weight dependence. In addition, the rate at which T_g drops with film thickness is, itself, a weak function of molecular weight, with the most dramatic shifts being associated with the largest molecular weights.

In contrast, regardless of the underlying model for local T_g as a function of film thickness, the result of performing a democratic average is that the overall film T_g is doomed to approach the bulk value with a $1/h$ dependence, which is a significantly slower approach than experimental data show. We therefore pursue an alternative, suggested by our simple treatment of the transition between glass and melt for layers plasticized by the presence of a free surface.

As a final introductory point, we raise the issue of molecular weight dependence for the case of supported films. There appears to be a fairly general consensus²⁴ that even down to extremely low molecular weights (on the order of 10^4 g/mol) there is no evidence of molecular weight dependence. A modest reading the literature does suggest a number of general observations. For example, the bulk glass transition temperatures appear to be achieved for films having thickness around 75 nm, regardless of the molecular weight of the sample.²⁴ It is also clear that the presence of a substrate has significant experimental impact, in that dramatic suppression of the glass transition only becomes evident for extremely thin films—those having thicknesses below about 20 nm. Films thicker than this only show shifts in T_g of about 5 K or less relative to their eventual bulk value. A complicating issue is that there also appears to be a rather significant dispersion of T_g values when results using different techniques from different laboratories are compared,²⁴ such that the uncertainty in T_g at any given film thickness is likely to be at least 5 K. It therefore becomes difficult to draw firm conclusions about possible molecular weight effects for films of

modest thickness when the precision is on the order of the effect. On the other hand, the thinnest supported films, i.e., the ones which show the most dramatic effects, have the complication of being under the influence of the substrates on which they are supported. Given that our model describes semi-infinite films, focusing on the effects of the free surface and not accounting for an underlying support, it becomes problematic to draw firm quantitative conclusions regarding issues such as molecular weight dependence. The one set of experimental data which provides a real opportunity for comparison has been collected for only one molecular weight. This means that a true test of our model results for semi-infinite films is yet to come, as we discuss further below.

The rest of the paper is divided as follows: In the next section we discuss how the model is used to create the theoretical equivalent of an experimental line shape, such as are often shown when ellipsometry measurements are carried out. In section 3, we discuss different possible routes to identifying the glass transition for a slice of film, and strategies for reporting an averaged T_g . In sections 4 and 5, we present results for semi-infinite and freestanding films. Finally, section 6 is devoted to our summary and conclusions.

2. Local Line Shape

The experiments described above measure the total film thickness as a function of temperature. The total film thickness is the sum of the thicknesses of each differential slice. The slices will in general have different local glass transition temperatures, and thus will contract by different amounts as the film is cooled.

We envision dividing the film into differential slices of equal mass per area, or equivalently of equal height dz at the bulk glass transition. (Above the bulk glass transition, the density everywhere in a freestanding film is equal, as no part of the film has yet become glassy.) We take as our reference length scale the root-mean-square radius of gyration of the longest loop, $N^*(T_g^b)$, which is effective at the bulk T_g^b . The chain length or molecular weight N^* of this longest mobile loop is a parameter in our model calculations.

In order to generate a local line shape, associated with a given differential slice, we write the change in total film thickness $\Delta h(T)$ as an integral over the relative change in local film thickness $\delta h(z, T)$, as

$$\Delta h(T) = \int_0^h dz \delta h(z, T) \quad (2)$$

in which h is the total film thickness at T_g , and $z = 0$ corresponds to the air–film interface. Note that $\delta h(z, T)$ is taken to depend on position z but not on the overall thickness of the film.

For small thickness changes, $\delta h(z, T)$ is given by the ratio of the change in local density $\delta \rho(z, T)$ to the density ρ_g at the bulk glass transition,

$$\delta h(z, T) = -\delta \rho(z, T)/\rho_g \quad (3)$$

We model the local relative changes in thickness $\delta h(z, T)$ phenomenologically, as follows. By definition, $\delta h(z, T_g^b)$ vanishes (we measure thickness relative to its value at T_g^b). Above the bulk glass transition, we are in the melt state, in which all portions of the film have the same thermal expansion coefficient α_m , assumed to be independent of temperature for simplicity.

At a temperature $T_g(z)$ at or below T_g^b , a differential slice at z undergoes its local glass transition, calculated in the companion paper (DOI 10.1021/ma101098d). Below $T_g(z)$, the slice is glassy, falling out of complete thermal equilibrium. A glassy slice loses

some formerly accessible vibrational modes, and its thermal expansion coefficient is reduced to some smaller value α_g . We assume each glassy slice to have the same α_g regardless of the value of $T_g(z)$, i.e., how suppressed the glass transition is for the slice, or how close it is to the free surface. The ratio α_g/α_m is an adjustable parameter in our model.

It remains to specify how $\delta h(z, T)$ changes between T_g^b and $T_g(z)$, in the “plasticized state”, made molten by the action of loops transporting kinks. First, we assume that all plasticized slices have the same density at a given temperature. Second, we assume that the thermal expansion coefficient of a slice at z is a smooth function of T above $T_g(z)$; in particular, there is no break in slope of $\delta h(z, T)$ at the bulk transition for a plasticized slice (for which $T_g(z)$ is distinctly less than T_g^b). So we may write

$$\delta h(z, T) = \begin{cases} \alpha_m(T - T_g^b) & T \geq T_g^b \\ \delta h(T) & T_g(z) < T < T_g^b \\ \alpha_g(T - T_g(z)) + \delta h(T_g(z)) & T \leq T_g(z) \end{cases} \quad (4)$$

In the above, $\delta h(T)$ is a “line shape function” that we must specify. It must have slope α_m at T_g^b for continuity with the melt. And, it must have slope α_g at T_0 , the minimum temperature at which we may still have any plasticized region. Finally, $\delta h(T)$ vanishes at $T = T_g^b$.

Our choice for the function $\delta h(T)$ determines how the thermal expansion coefficient of the plasticized material decreases with temperature. This decrease corresponds to a gradual withdrawal of some of the vibrational modes that would have become inaccessible at T_g^b , but were preserved by the plasticizing action of the loops. Here we assume a smooth linear transition of $\alpha(T)$ between values α_m at T_g and α_g at T_0 ; this leads to

$$\delta h(T) = \alpha_m(T - T_g^b) + \alpha_g \frac{(T - T_0)^2 - (T_g^b - T_0)^2}{2(T_g^b - T_0)} \quad (5)$$

Our specification of $\delta h(z, T)$ differs from the cartoon proposed by de Gennes,^{1,2} who posited that the plasticized state would have a constant thermal expansion coefficient α_p , with a value intermediate between α_m and α_g . That simplified model would however lead to a sharp transition at T_g^b , at which the thermal expansion coefficient jumped from α_m to α_p throughout the film. Such a transition has not been reported, which is part of the motivation for our proposal.

3. Locating the Transition

As illustrated in the companion paper to this, different slices in a film undergo their local glass transition at different temperatures. These local glass transitions are presumed sharp, with a break in slope of $\delta h(z, T)$ at $T_g(z)$. However, the change in total film thickness $\Delta h(T)$ will not display a sharp glass transition, because

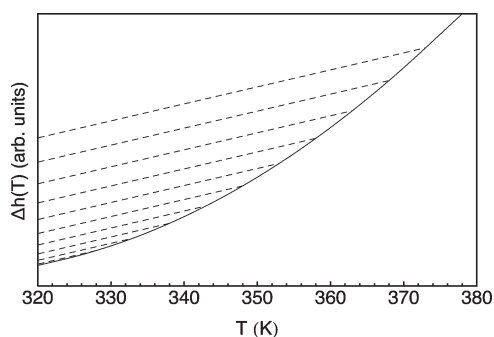


Figure 1. Representative curves for $\delta h(z, T)$ (with break in slope, dashed below $T_g(z)$), for a series of thin slabs contributing to the overall $\Delta h(T)$ (solid curve).

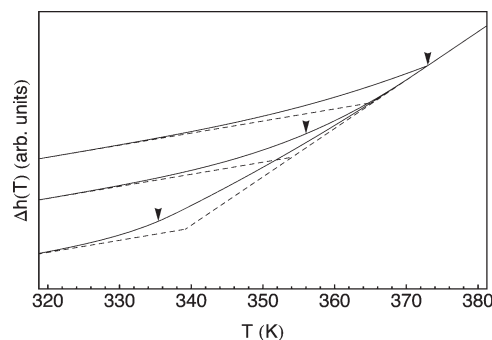


Figure 2. Representative curves for $\Delta h(T)$, together with tangents at $T = T_0$ and $T = T_g$ (dashed), and markers for “mid-slope” points. Curves offset for clarity. Values of h/h^* equal to 0.1, 0.6, and 1.5. Chain length $N = N^*$; other parameters as in main text ($c = 8$, $T_0 = 273$ K, $\alpha_g/\alpha_m = 0.25$).

the constituent slices have their local transitions at different temperatures $T_g(z)$.

In Figure 1, we illustrate how local transitions for a series of slices within a film combine to yield a prediction for the dependence of overall film thickness on temperature. Each of the dashed lines shows thickness versus temperature for a single slice. The progression of dashed lines from top to bottom illustrates the effect of slice position, ranging from deep in the film (topmost) to a slice at or near the surface (bottom most). Note that the curve for the deepest slice has the most marked change in slope at the transition. This slice is positioned deep enough that the temperature needed to melt the material is near that of the bulk glass transition. Conversely, the bottom dashed curve in the set exhibits the weakest transition, in the sense of slope change, at the lowest temperature. This is associated with a slice close to the surface, where the local glass transition has been deeply depressed.

A straightforward averaging of the contributions from each, equivalent, slice, would yield a single curve. Three examples of such curves are shown in Figure 2, which illustrates the results for three choices of the overall film reduced thickness h/h^* , where the characteristic length h^* is the radius of gyration of a chain segment of length N^* . (In generating the curves of Figure 2, we have chosen representative values of our adjustable parameters $c = 8$, $T_0 = 273$ K, $\alpha_g/\alpha_m = 0.25$, which we maintain throughout the rest of the paper.)

This plot is analogous to what an experimentalist would obtain on three such samples using, for example, ellipsometry or fluorescence methods. In analogy with the experimental analysis, we must now specify how a single transition temperature is to be assigned for a freestanding film of thickness h . Experimentalists commonly fix a transition temperature over some range of T , by drawing a tangent to the data on each end of the data set and finding the intersection point of the two tangents. The question arises: how wide in T should the data set be taken, and where should the tangents be drawn?

Informed by the present model, the logical places to draw the two tangents are (1) at the bulk glass transition T_g^b , where the entire film must have the melt thermal expansion coefficient α_m , and (2) at the Vogel temperature³ T_0 for the slip motion, where the entire film must have the glass thermal expansion coefficient α_g . Of course, for the experimenter the lower tangent poses a problem, because we do not know a priori where T_0 is; T_0 for slip motion need not be the same as the value for the bulk glass transition. Still, the essence of our tangent prescription is to take the upper tangent where the thermal expansion coefficient matches the known value α_m for the bulk melt, and take the lower tangent where the thermal expansion coefficient matches the known value α_g for the bulk glass.

In the theory, of course, it is straightforward to implement this procedure for locating the crossing point of the two tangents. Below T_0 , eqs 2 and 4 give a linear behavior for $\Delta h(T)$, namely

$$\Delta h(T) = \int_0^h dz (\delta h(T_g(z)) + \alpha_g(T - T_g(z))) \quad (6)$$

Above T_g^b we again have a linear result, $\Delta h(T) = h\alpha_m(T - T_g^b)$. Thus, above T_g^b and below T_0 , the function $\Delta h(T)$ is its own tangent. Equating these two expressions determines the crossing point $T_{g,tan}$ of the tangents. We define $\Delta T_{g,tan}(h)$ equal to $T_{g,tan}(h) - T_g^b$, the shift of the apparent glass transition relative to bulk.

A modest amount of algebra reveals that determination of the glass transition via the intersection of the two tangents described above is identically equivalent to taking the unweighted, “democratic”, average of the local glass transitions in the film.

$$\Delta T_{g,tan}(h) = \frac{1}{h} \int_0^h dz \Delta T_g(z) \quad (7)$$

In other words, averaging the transition over the total set of slices within the film yields the exact result of the limiting tangents associated with the melt and sub-Vogel temperature glass.

An important distinction can be made between films thick enough to have an interior region that is not plasticized (and therefore becomes glassy at T_g^b , and so has local $\Delta T_g(z) = 0$), and films thin enough that all portions of the film are plasticized to some extent. We call the former case “sandwich” films, with the “meat” being the interior unplasticized region and the “bread” the plasticized portions on either face of the film. For sandwich films, only the two “bread” regions contribute to the integral of eq 7. Then the average $\Delta T_{g,tan}$ becomes:

$$\Delta T_{g,tan}(h) = \frac{2}{h} \int_0^{h_{max}} dz \Delta T_g(z) \quad (8)$$

Here h_{max} is the maximum depth into the film that is ever plasticized, i.e., $T_g(h_{max})$ equals T_g^b . (The factor of 2 in front arises from the two “slices of bread”.)

In Figure 2, we show the three sets of tangents. That associated with each trace above the melt T_g has been drawn in red, and is the same in all three cases. The tangent associated with the trace below T_0 has the same slope in each case, of course, but occurs in a different position, reflecting the different temperature at which the overall film went glassy. The three different intersection points of the sets of tangents would therefore be the estimates using this approach for the overall film T_g reported for each of three the respective thicknesses. Three arrows are also indicated in the figure, and we will come back to these shortly.

Now consider the dependence of $\Delta T_{g,tan}(h)$ defined by eq 8 on total film thickness h . We of course expect that for sufficiently thick films, the average transition temperature $T_{g,tan}(h)$ should approach the bulk transition T_g^b , hence $\Delta T_{g,tan}(h)$ should approach zero. However, it is apparent from eq 8 that $\Delta T_{g,tan}(h)$ approaches zero slowly, as $1/h$. Thus, a plot against film thickness of T_g values obtained as illustrated in Figure 2, from the intersection points of the tangent lines, would show a clear $1/h$ dependence.

In contrast, the reported values for glass transition temperatures from ellipsometry experiments as a function of film thickness show an sharp crossover to the bulk T_g^b value, not a slow $1/h$ approach. Note however that the experimenters do not systematically report their line shapes, nor do they draw their tangents at a standard temperature; it may well be possible to get rather different results for the transition temperature depending on where the tangents are drawn.

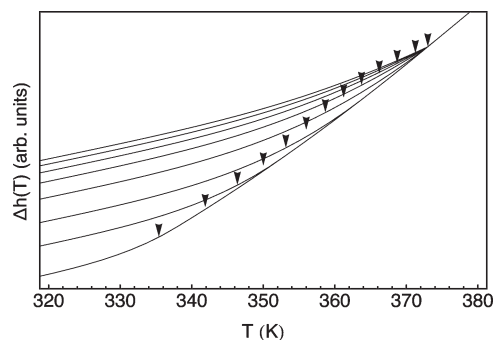


Figure 3. Family of curves for semi-infinite film top labeled layer $\Delta h(T)$ versus temperature, for $h/h^* = 0.1, 0.3, \dots, 1.5$ and $N = N^*$. Other parameters as in main text ($c = 8$, $T_0 = 273$ K, $\alpha_g/\alpha_m = 0.25$).

The route just described for determining the averaged T_g of a film as a function of thickness therefore has several disadvantages. We thus seek an alternative, albeit still well-defined, route to the averaged transition. We note in passing the implication that the result will no longer represent a “democratic” weighting of the local transitions.

Recall that we chose a linear transition in thermal expansion coefficient between bulk melt and glass values. A rather straightforward alternative route is therefore to identify the glass transition temperature as that associated with a tangent to the curve having slope exactly halfway between the melt and the glass slopes. (This approach has been used by at least some experimenters, including Keddie et al.¹¹) Results for the three sample curves in Figure 2 are indicated by solid arrows; the locations of the transitions appear to be close to what the eye would choose as the most noticeable “break” in the trace.

We have now elaborated how our model may be used to generate the equivalent of experimental thickness-temperature traces for thin films, as well as a protocol for identifying the averaged film glass transition. In the sections that follow, we apply this approach to generate results for semi-infinite and freestanding films.

4. Results for Semi-Infinite Films

As discussed in the Introduction, experiments exist that in effect measure the glass transition temperature averaged over a labeled “reporting layer”. In one set of experiments, a labeled thin layer is placed atop an unlabeled thick supported film; the thickness h of the labeled layer is varied, and average $T_g(h)$ values reported.²³ We idealize this situation by regarding the underlying thick film as infinitely thick; thus we are interested in the average T_g of the topmost thickness h of a semi-infinite film. We apply the averaging process of the previous section to this new configuration.

Figure 3 displays representative curves for $\Delta h(T)$, the change in thickness of the topmost “labeled” portions of semi-infinite films made from an infinite molecular weight polystyrene (PS). The thickness h of the labeled portions are reported in units of h^* , which (as in the previous section) denotes the radius of gyration of a chain of length N^* . Recall that N^* is the longest possible active loop, given by the relation $N^* = N^*(T_g^b)$ at T_g^b .

As in the companion paper (DOI 10.1021/ma101098d), we choose N^* to be 2.0×10^6 g/mol, which sets the limit for the longest effective loop length in an infinite molecular weight sample. This particular choice is motivated by observing that for PS of extremely high molecular weight (certainly by 9.1×10^6 g/mol) the bulk glass transition is achieved for films having thicknesses of roughly 95 nm and greater.

As noted in the figure caption, h/h^* ranges from 0.1 to 1.5. For the choice of N^* noted above, h^* is a length of 38 nm. Thus, the labeled film thicknesses presented in Figure 3 range from 3.8 to 57.0 nm.

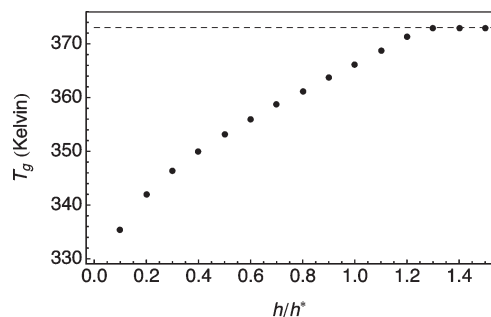


Figure 4. Glass transition temperature T_g versus h/h^* , as inferred by “mid-slope” criterion, corresponding to results of Figure 3.

As described above, we identify the transition as occurring at the temperature associated with a tangent line having a slope halfway between that of the glassy and melt regions. The set of resulting transition temperatures is indicated in the figure by black arrows.

In Figure 4, we map the results of Figure 3 to create a plot for the infinite molecular weight sample of the shift in $T_g(z)$ from the bulk value of 373 K as a function of relative film thickness. Once again, the abscissa is shown in reduced units, where the reduction parameter is the root-mean-squared radius of gyration of a chain of length N^* (T_g^0), chosen here to be 2.0×10^6 g/mol. Thus, the abscissa represents film thicknesses out to 57.0 nm, at which point $h = 1.5h^*$. As the figure shows, the theoretical predictions are reasonable both for the degree of T_g depression, as well as for the relative length scale over which it occurs. Equally important, the model results exhibit a notable drop in T_g for films having thickness less than about 52 nm, with a subsequent shift in temperature of roughly 30 K over a change in film thickness of only 30 nm. This is qualitatively consistent with experimental observations,²⁴ and distinctly different than the slower, $1/h$ -like drift which is the result of the so-called “democratic averaging” process discussed previously.

In semi-infinite films only one free surface is present, and there are no interactions with a substrate. Experimental implementation of this arrangement has been realized in the work of Torkelson et al. (see Figure 2 of ref 23), which includes results for a labeled surface reporting layer of variable thickness resting on a “silent” (i.e., unlabeled) very thick (240–270 nm) layer of the same polymer loaded onto a substrate. Observed differences from the bulk glass transition can thus be attributed solely to the influence of the film/air interface. Similarly, our model for the semi-infinite film reflects only the presence of one free surface.

Although the theoretical result for the probability that a segment is a particular distance away from the surface differs in the semi-infinite case, relative to that for the finite film (cf. eqs 12 and 13 in the companion paper (DOI 10.1021/ma101098d), the model predicts a similar sensitivity to molecular weight. In Figure 5, we show the effect of changing molecular weight on the range and extent of the T_g shift; as the figure caption indicates, the molecular weights are in reduced units, with the reduction parameter being the value of N^* . Choosing the value of N^* to be 2.0×10^6 g/mol would therefore translate the results in Figure 5 to be associated with molecular weights, from left to right, of 4.0×10^5 , 8.0×10^5 , 1.2×10^6 , 1.6×10^6 , and 2.0×10^6 g/mol. For the two largest molecular weight model samples the limits of plasticization have essentially been reached, and moving to still higher molecular weights would produce negligible change.

Experimental data points illustrating the whole-film T_g shift in supported films are somewhat scattered, as Figure 1 in the recent paper by Torkelson et al. illustrates.²⁴ However, the cumulative results generally support the notion that PS thin films on silicon oxide substrates exhibit thickness-related shifts in the glass

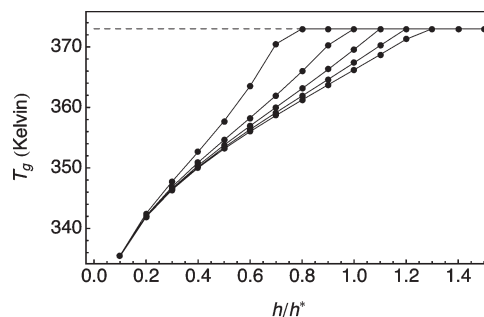


Figure 5. Glass transition temperature T_g versus labeled top layer thickness h/h^* for semi-infinite films, for a family of different molecular weights $N/N^* = 0.2, 0.4, 0.6, 0.8, 1.0$. Other parameters as in main text ($c = 8$, $T_0 = 273$ K, $\alpha_g/\alpha_m = 0.25$).

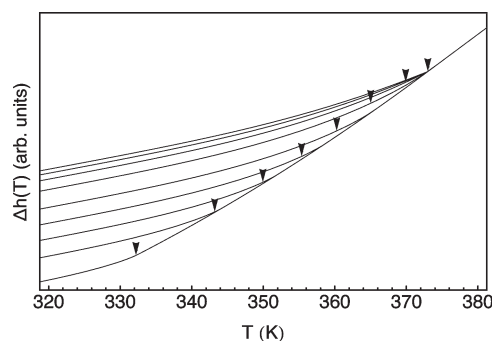


Figure 6. Family of curves for freestanding film $\Delta h(T)$ versus temperature, for $h/h^* = 0.2, 0.6, \dots, 3.4$ and chain length $N = N^*$. Other parameters as in main text ($c = 8$, $T_0 = 273$ K, $\alpha_g/\alpha_m = 0.25$).

transition that are essentially independent of molecular weight. We note, though, that the right experiments have not yet been done to determine whether this insensitivity to molecular weight is evident even when only a slice of the film adjacent to the free surface is reporting. In this sense our model predictions have yet to be tested.

5. Results for Freestanding Films

As noted in the Introduction, experimental results illustrating the effect of film thickness on the glass transition of freestanding films of varying molecular weight show striking trends^{15,29} (see in particular Figure 4 of Dalnoki-Veress et al.¹⁵). In Figure 6, which is the analogue of results for the semi-infinite case given in Figure 3, the shift in glass transition for a series of freestanding PS film of infinite molecular weight is indicated by the series of arrows. This set of temperature-thickness results represents what would be obtained as the limiting set of points in Figure 7 which, in fact, shows results for a series of finite molecules weights. As in Figure 7, the molecular weights are scaled relative to the value of N^* , such that the choices represented in the figure correspond (using 2.0×10^6 for N^*) to values of (from left to right) 4.0×10^5 , 8.0×10^5 , 1.2×10^6 , 1.6×10^6 , and 2.0×10^6 g/mol.

There are both notable similarities and differences in comparing the model results to those of experiment. Before detailing these, we emphasize that we have not tried to optimize agreement with experiment in generating the results of Figure 7; the PS-related parameters are the same as those used in producing results for the semi-infinite films of varying molecular weights.

Even given comparable shifts in temperature over comparable length scales it is clear that there are conceptual differences between the model predictions and the DV set of experimental data.¹⁵ According to the theory, plasticization in sufficiently thin films becomes independent of molecular weight. For example, the model predicts that a freestanding film of 20 or 30 nm thickness

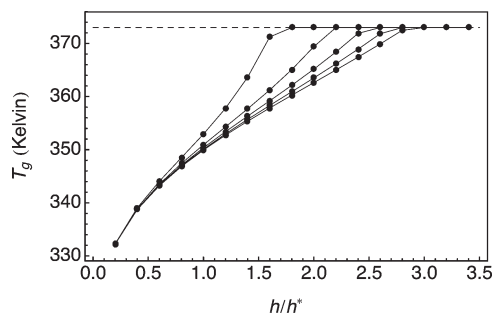


Figure 7. Glass transition temperature T_g versus freestanding film thickness h/h^* , for a family of different molecular weights $N/N^* = 0.2, 0.4, 0.6, 0.8, 1.0$. Other parameters as in main text ($c = 8$, $T_0 = 273$ K, $\alpha_g/\alpha_m = 0.25$).

will be plasticized equivalently for a sample of, e.g., 300 000 g/mol as for one of 3 000 000 g/mol. This means that our “fan” of molecular-weight dependent lines coalesce at a point associated with small length and low temperature. This does not match the DV data¹⁵ which fan in the opposite direction, the lines coalescing at a putative temperature higher than the bulk T_g , and distance larger than the thickest film for which experimental T_g suppression is observed.

The pattern in the experimental data is impressively clear, yet we remain puzzled by the evident sensitivity of the film results at low length scales to the molecular weight of the sample. For example, from the DV data¹⁵ we see that a film of 40 nm thick shows a T_g suppression of about 40 K for a sample of 5.75×10^5 g/mol, compared to a 70 K shift for a sample of 1.25×10^6 g/mol. In both cases, the film is significantly thicker than the root-mean-squared radius of gyration, which would be roughly 20 nm for the former and 30 nm for the latter. In addition, considering the thicker samples in the study, why does the film T_g drop so much more precipitously from the bulk value for the highest molecular weight samples, relative to the behavior for the lowest molecular weight? Answers remain elusive, however, we can certainly conclude that accounting for plasticization through transmission of free volume along chain loops does not capture these particular aspects of whatever physical phenomena the data reflect.

6. Summary and Conclusions

More than a dozen years have passed since the initial reports of a shift in the polymeric glass transition temperature for material in a thin film, relative to the bulk. Early experiments focused on supported films, however, much of the recent research has targeted freestanding films. The range in configurations—from examining multicomponent layers, to the effect of embedded nanoparticles—as well as the increasing breadth of experimental techniques have resulted in the creation of a field which is more blessed by data than by understanding. This paper, along with the preceding one, as well as recent (unrelated) work which develops a percolation treatment for the local glass transition in supported thin films,⁴ represent our own efforts to bridge the rapidly widening gap between experimental results and theoretical insight.

Our earlier study on supported thin films,⁴ which was the first paper to generate model results for the profile of local glass transitions, lead us to conclude that a percolation treatment was capable of capturing the effect of an attractive substrate on both the local and averaged glass transition. On the other hand the predictions, while reflecting the independence of sample molecular weight on experimental results, also made clear that the depression of T_g observed close to the surface could not be accounted for solely by a reduction in the number of percolating paths linking isolated glassy clusters to the globally glassified layer adjacent to the substrate.

In this two-paper study, we create (in the first paper (DOI 10.1021/ma101098d) and implement (here) the delayed glassification (DG) model, which brings to life in a clear and substantive way the notion, first suggested by de Gennes,^{1,2} that a free surface may serve as source and sink for segmental-sized “kinks” of free volume. Using this “slip” mechanism in our DG model, the kinks, created and destroyed at the film-surface interface, propagate into film by traveling along polymeric loops. A loop that is too long is no longer effective at helping to plasticize the film; the “effective” loop length is temperature-dependent. One parameter in the model is N^* , the limiting effective loop length which is still active at the bulk T_g . At lower temperatures, we have assumed a WLF-like form for $N^*(T)$, thereby introducing two additional parameters: the associated energy parameter, A , and limiting temperature, T_0 . Finally, we use an exponential distribution to account for the effect of finite molecular weight. This modifies the probability that a loop may be active, since a kink encountering a chain end will no longer be able to propagate.

The DG model accounts for some, but not all, of the physics revealed through experiment. We find a dramatic drop in the glass transition, relative to the bulk value as film thickness diminishes. Both the rate at which the glass transition is suppressed as a function of thickness, as well as the critical thickness at which this occurs, depends on molecular weight. At high enough molecular weights the effects saturate, and further increases have no additional effect. We depart from experiment¹⁵ in finding that molecular weight differences vanish for ultrathin films, where the extent of T_g suppression becomes molecular weight independent. We also find that the suppression of the glass transition for semi-infinite films is dependent on the molecular weight of the sample in a way which is analogous to that of free-standing films. These predictions remain to be tested, as current data on T_g suppression in the presence of a single air interface involve films supported by a substrate.

We emphasize that any theoretical approach that predicts local glass transition temperatures in a thin polymer film, will be confronted with the need to supply some sort of average T_g value to compare to experiment. Many averages are possible to compute, the most obvious being a “democratic” weighting of the local T_g values from each differential slice of material. However, it appears from our analysis that this “democratic average” does not correspond well to what experimenters typically report. This theoretical caveat does not depend on the validity of the DG model.

In summary, we hope that these results are provocative enough to generate new data, and look forward to revisiting the challenges of understanding these systems as new experimental evidence of the physics involved is revealed.

References and Notes

- (1) de Gennes, P. *Eur. Phys. J. E* **2000**, 2, 201–205.
- (2) de Gennes, P. *C. R. Acad. Sci. Paris Ser. IV* **2000**, 1, 1179–1186.
- (3) Ferry, J. D. *Viscoelastic properties of polymers*; Wiley: New York, 1980.
- (4) Lipson, J. E. G.; Milner, S. T. *Eur Phys J B* **2009**, 72, 133–137.
- (5) Fukao, K.; Miyamoto, Y. *Europhys. Lett.* **1999**, 46, 649–654.
- (6) Fukao, K.; Miyamoto, Y. *Phys. Rev. E* **2000**, 61, 1743–1754.
- (7) Forrest, J.; DalnokiVeress, K.; Stevens, J.; Dutcher, J. *Phys. Rev. Lett.* **1996**, 77, 2002–2005.
- (8) Forrest, J.; DalnokiVeress, K.; Dutcher, J. *Phys. Rev. E* **1997**, 56, 5705–5716.
- (9) Mattsson, J.; Forrest, J.; Borjesson, L. *Phys. Rev. E* **2000**, 62, 5187–5200.
- (10) Fryer, D.; Peters, R.; Kim, E.; Tomaszewski, J.; de Pablo, J.; Nealey, P.; White, C.; Wu, W. *Macromolecules* **2001**, 34, 5627–5634.
- (11) Keddie, J.; Jones, R.; Cory, R. *Faraday Discuss* **1994**, 98, 219–230.
- (12) Kim, J.; Jang, J.; Zin, W. *Langmuir* **2001**, 17, 2703–2710.
- (13) Roth, C. B.; Pound, A.; Kamp, S. W.; Murray, C. A.; Dutcher, J. R. *Eur Phys J E* **2006**, 20, 441–448.
- (14) Roth, C. B.; Dutcher, J. *Eur. Phys. J.* **2003**, 12, S103–S107.

- (15) Dalnoki-Veress, K.; Forrest, J. A.; Murray, C.; Gigault, C.; Dutcher, J. R. *Phys. Rev. E* **2001**, *63*, 031801.
- (16) Dalnoki-Veress, K.; Forrest, J. A.; de Gennes, P. G.; Dutcher, J. R. *J. Phys. IV Fr.* **2000**, *10*, 221–226.
- (17) Sharp, J.; Forrest, J. *Phys. Rev. Lett.* **2003**, *91*, 235701.
- (18) Tsui, O.; Zhang, H. *Macromolecules* **2001**, *34*, 9139–9142.
- (19) Miyazaki, T.; Nishida, K.; Kanaya, T. *Phys. Rev. E* **2004**, *69*, 061803.
- (20) Tsui, O.; Russell, T.; Hawker, C. *Macromolecules* **2001**, *34*, 5535–5539.
- (21) Miyazaki, T.; Inoue, R.; Nishida, K.; Kanaya, T. *Eur. Phys. J.* **2007**, *141*, 203.
- (22) Ellison, C.; Kim, S.; Hall, D.; Torkelson, J. *Eur Phys J E* **2002**, *8*, 155–166.
- (23) Ellison, C.; Torkelson, J. *Nat. Mater.* **2003**, *2*, 695–700.
- (24) Kim, S.; Hewlett, S. A.; Roth, C. B.; Torkelson, J. M. *Eur. Phys. J. E* **2009**, *30*, 83–92.
- (25) Priestley, R.; Ellison, C.; Broadbelt, L.; Torkelson, J. *Science* **2005**, *309*, 456–459.
- (26) Ellison, C.; Mundra, M.; Torkelson, J. *Macromolecules* **2005**, *38*, 1767–1778.
- (27) Mundra, M.; Ellison, C.; Rittigstein, P.; Torkelson, J. *Eur. Phys. J. Spec. Top.* **2007**, *141*, 143.
- (28) Priestley, R.; Mundra, M.; Barnett, N.; Broadbelt, L.; Torkelson, J. *Aust. J. Chem.* **2007**, *60*, 765.
- (29) Miyazaki, T.; Inoue, R.; Nishida, K.; Kanaya, T. *Eur. Phys. J. Spec. Top.* **2007**, *141*, 203–206.